measurements of bottom-current speed are unavailable in the ISW region, a flow speed of 7 cm s^{-1} was assumed, on the basis of measurements of outflow from the Filchner Depression, to the southeast of the ISW region (*15*). To account for the observed increase in the thickness of the benthic layer, we used average thickness values of 70 and 240 m for the regions south and north of 66°S, respectively. As a consequence of this subdivision, 30% of the estimated shelf-water contribution originates from the area north of 66°S.

Data collected from the upper water column during ISW reveal that a narrow band of T_{max} water >0.5°C flowed along the western edge of the Weddell Sea over the continental slope (Fig. 4). This feature may extend from its first appearance near the Greenwich Meridian (*16*) covering a distance of 2000 km. Cooling of the T_{max} layer en route from near 1.0°C at the Greenwich Meridian to 0.5°C at the northern end of the ISW data array represents attenuation by vertical and isopycnal processes that expose the WDW core to cold surface and continental-shelf water masses. In the western Weddell, a more stable layer within the pycnocline is observed in the 200- to 300-m interval, with the WDW T_{max} at 500 to 600 m. This stands in sharp contrast to the shallow (at the base of the winter mixed layer near 110 m) pycnocline and the warmer T_{max} (>0.8°C within the 150- to 250-m interval) of the eastern section of the Weddell Gyre (*3*). This stratification difference may account for different vertical heat fluxes observed in the two regimes (*3, 17*) and associated perennial ice cover of the western Weddell.

With the Weddell Gyre's center well east of the ISW survey, generally between 20° and 40°W (*2*), the baroclinic expression of the western boundary current appears to be over 400 km wide. However, the distribution of the T_{max} along the western rim of the Weddell Gyre distinguishes two components of the western boundary current: A rim current that advects the warmest water from the eastern margins of the gyre to the western edge and a longer residence interior component, basically a recirculation of the inner hub of the gyre (*16, 18*). The rim current is likely to be more important to the overall water-mass formation processes, as it provides the salt required for bottom-water formation to the continental margins. Determination of geostrophic shear with the thermal wind equation, with adjustment to the order of the current speed observed in the near-surface layer at ISW (*19*), indicates that the rim-current transport is about 10 × 10^6 m^3 s^{-1} to 15 × 10^6 m^3 s^{-1}. The interior recirculation flow is unknown, but it may be larger than 10 × 10^6 m^3 s^{-1}: with a mean bottom-current speed of 1.3 cm s^{-1} as a reference, as measured at 66°30′S and 41°W (*20*), transport of over 30 × 10^6 m^3 s^{-1} is likely, producing a total western boundary transport of about 40 × 10^6 m^3 s^{-1}.

REFERENCES AND NOTES

1. G. E. R. Deacon, *Deep-Sea Res.* **26**, 981 (1979).
2. A. Orsi, W. Nowlin, T. Whitworth, *ibid.* **40**, 169 (1993).
3. A. Gordon and B. Huber, *J. Geophys. Res.* **95**, 11655 (1990).
4. E. Shackleton, *South* (MacMillan, New York, 1920).
5. N. Bagriantsev, A. Gordon, B. Huber, *J. Geophys. Res.* **94**, 8331 (1989).
6. V. V. Gouretski and A. I. Danilov, *Deep-Sea Res.* **40**, 561 (1993).
7. T. Foster and E. Carmack, *ibid.* **23**, 301 (1976).
8. P. Schlosser, personal communication.
9. A. Foldvik, T. Gammelsrød, T. Tørresen, *Antarct. Res. Ser.* **43**, 5 (1985).
10. A. Gill, *Deep-Sea Res.* **20**, 111 (1973).
11. Cabbeling refers to the mixing of two parcels of seawater with different temperature and salinity but similar densities. Because of the nonlinear equation of state for seawater, such mixtures can produce a parcel that is denser than the two constituent parcels. Thermobaricity is a property of seawater at temperatures below which the compressibility of seawater is significant in the determination of its density. As a parcel of water at sufficiently low temperature is subject to increasing pressure, it is compressed and can therefore sink.
12. This isotherm falls well within the linear *T-S* segment and hence is above the influence of the local benthic layer. The average potential temperature of the deep and bottom water below the 0.2°C isotherm decreases by 0.25°C from station 64 to station 70, coinciding with a thickening of the benthic layer. The corresponding salinity is reduced by 0.015 psu. This suggests additional injection of WSBW into the benthic layer north of 66°S.
13. E. Carmack, in *A Voyage of Discovery* (Pergamon, New York, 1977), pp. 15–42.
14. ______, *Deep-Sea Res.* **21**, 431 (1974).
15. A. Foldvik, T. Kvinge, T. Tørresen, *Antarct. Res. Ser.* **43**, 21 (1985).
16. T. Whitworth and W. Nowlin, *J. Geophys. Res.* **92**, 6462 (1987).
17. M. McPhee, J. Morison, D. Martinson, *Eos* **73**, 308 (1992).
18. A. Gordon, in *Antarctic Ocean and Resources Variability* (Springer-Verlag, Berlin, 1988).
19. R. Muench, J. Gunn, M. Morehead, *Eos* **73**, 301 (1992).
20. T. Foster and J. Middleton, *Deep-Sea Res.* **26**, 743 (1979).
21. J. Labrecque and M. Ghidella, *J. Geophys. Res.*, in press.
22. Funded by NSF grant DPP 90-24577. We thank J. Ardai, R. Guerrero, G. Mathieu, S. O'Hara, and R. Weppernig for help collecting the CTD data, and W. Haines and P. Mele for data processing. This is contribution 5101 of Lamont-Doherty Earth Observatory.

28 April 1993; accepted 15 July 1993

Pressure-Induced Enhancement of T_c Above 150 K in Hg-1223

M. Nuñez-Regueiro,* J.-L. Tholence, E. V. Antipov, J.-J. Capponi, M. Marezio†

The recently discovered homologous series $HgBa_2Ca_{n-1}Cu_nO_{2n+2+\delta}$ possesses remarkable properties. A superconducting transition temperature, T_c, as high as 133 kelvin has been measured in a multiphase Hg-Ba-Ca-Cu-O sample and found to be attributable to the Hg-1223 compound. Temperature-dependent electrical resistivity measurements under pressure on a (>95%) pure Hg-1223 phase are reported. These data show that T_c increases steadily with pressure at a rate of about 1 kelvin per gigapascal up to 15 gigapascals, then more slowly and reaches a T_c = 150 kelvin, with the onset of the transition at 157 kelvin, for 23.5 gigapascals. This large pressure variation (as compared to the small effects observed in similar compounds with the optimal T_c) strongly suggests that higher critical temperatures could be obtained at atmospheric pressure.

In analogy with the Bi- and Tl-based superconducting copper oxides, the structures of the $HgBa_2Ca_{n-1}Cu_nO_{2n+2+\delta}$ series are constructed with *n* CuO_2 layers sandwiched between rock-salt (BaO)(HgO_δ)(BaO) blocks. In comparison with the former, the Hg compounds yield noticeably higher conducting/superconducting transition temperatures, namely 94, 129, 133, and 126 K for the *n* = 1, 2, 3, and 4 compounds, respectively (*1–3*). The synthesis of the compounds is complicated by the low decomposition temperature of HgO. High pressure hinders this decomposition and facilitate the formation reactions. However, it is still not clear if the measured values of T_c are optimal. Besides the empirical method of changing the preparation conditions and stoichiometry, there is another way of checking this. It is now generally accepted (*4–6*) that application of high pressures up

M. Nuñez-Regueiro and J.-L. Tholence, Centre de Recherches sur les Très Basses Températures, CNRS-UJF, BP 166 Cedex 9, 38042 Grenoble, France.
E. V. Antipov, Department of Chemistry, Moscow State University, 119899 Moscow, Russia.
J.-J. Capponi and M. Marezio, Laboratoire de Cristallographie, CNRS-UJF, BP 166 Cedex 9, 38042 Grenoble, France.

---

*On leave of absence from Centro Atómico Bariloche, 8400 Bariloche, Argentina.

†Also at AT&T Bell Laboratories, Murray Hill, NJ 07974.

Fig. 1. AC susceptibility measurement of the Hg-1223 sample before compression, showing that at least 95% of the sample corresponds to the phase with $T_c \sim 133$ K.

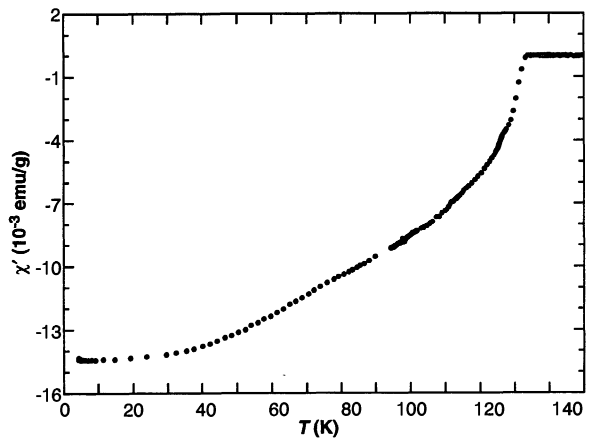

Fig. 2. Resistance of the sample under a pressure of 0.92 GPa. The resistance does not go to zero below T_c, possibly because of a light degradation of the surface of the finely ground grains of the compacted powder Hg-1223 sample.

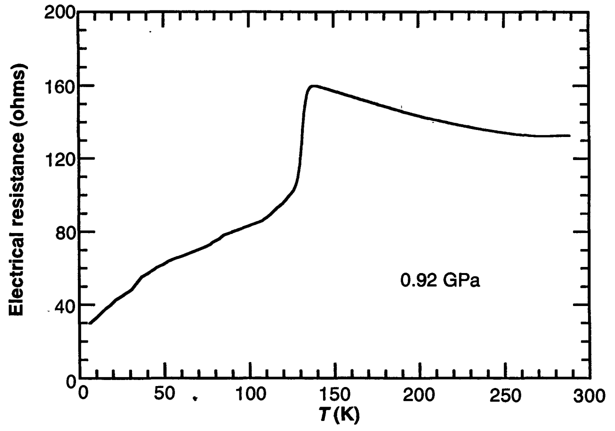

Fig. 3. Superconducting transition of Hg-1223 for different pressures as monitored by its electrical resistance (normalized to the value at 165 K).

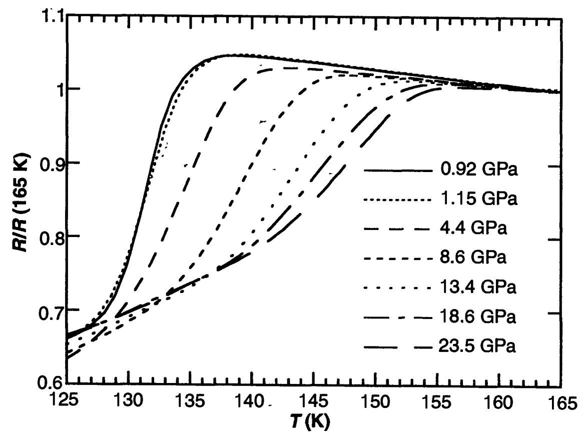

Fig. 4. Dependence of the superconducting transition temperature. $T_{c\ onset}$ is defined as the temperature at which the resistance turns visibly away from the high temperature behavior. $T_{c\ half}$ corresponds to the temperature halfway between 80% and 20% of the resistive transition. Horizontal error bars denote the pressure gradient in the cell, as monitored by the width of the superconducting transition of the lead manometer. The vertical error bars show the width of the superconducting transition.

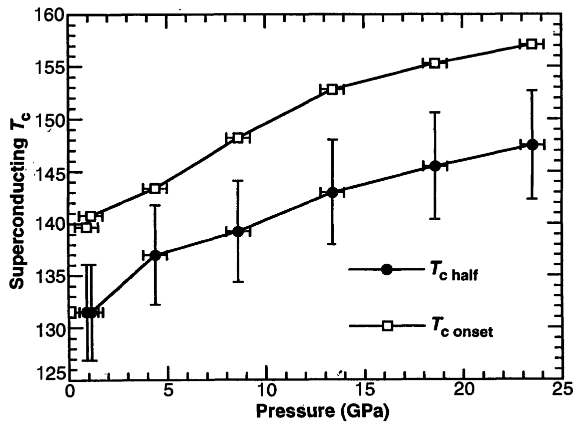

to ~20 GPa on an underdoped hole copper oxide superconductor may lead to a continuous increase of T_c, whereas compression of an overdoped sample causes a decrease and almost no effect is seen when the sample has the optimal composition. Therefore, we have measured the resistance of the Hg-1223 material under high pressure.

A large quantity (1 cm^3) of 95% pure Hg-1223 phase has been prepared for neutron diffraction experiments (7). A correct estimate of the superconducting volume has been made by AC susceptibility measurements on a finely ground powder, in order to avoid large current loops which in ceramic samples result in overestimated superconducting volume fraction. Only one clear superconducting transition was observed corresponding to at least 95% of the sample (Fig. 1). The same fraction of Hg-1223 was estimated from the neutron scattering measurements (7).

After a month in a dessicator, a small amount of the measured material was compacted into a sample with the approximate size of 0.7 mm by 0.3 mm by 0.03 mm, introduced into the pressure cell, and compressed at room temperature. The Bridgman diamond-anvil cell and the measuring apparatus have been described previously (8). A typical resistance curve is shown in Fig. 2. The resistivity measurements show that the compacted powder nature of the sample introduces a series resistance that hinders a zero resistance state for the overall sample. However, the superconducting transition is clearly seen and its width is easily determined.

We show in Fig. 3 a detail around the superconducting transition of the temperature dependence of the sample resistance at different pressures, normalized to the value at 165 K. The increase of the transition temperature with pressure is clearly seen. As is customary in resistivity measurements, we define two transition temperatures. The first, $T_{c\ onset}$, is the temperature at which the resistance visibly turns away from the behavior it shows at higher temperatures. Some authors (9) have proposed that this value could correspond to a different phase or doping concentration. The second, $T_{c\ half}$, is the temperature at halfway between 80% and 20% of the superconducting transition. At the lowest pressures it is slightly smaller than the value (133 K) of the onset of diamagnetism in the AC susceptibility measurements. We show in Fig. 4 the variation of these two T_c's with pressure. We observe that both increase steadily with pressure in a similar manner, meaning that $T_{c\ onset}$ most probably does not correspond to another phase but is rather due to the typical rounding, caused by thermodynamic fluctuations (as shown by the error bars in the figure, the pressure gradient cannot explain the observed transition width). Interestingly, we see that it continues to increase up to the highest pressure, meaning that the optimal structural arrangement has not been reached, and that the sample does not degrade under pressure. One can distinguish two regions, one below 15 GPa in which a large increase rate of $\sim$1 K/GPa is observed and one above with a smaller rate of $\sim$0.5 K/GPa.

Furthermore, if the increase of the resistance with decreasing temperature (see Fig. 2), is attributed to Hg-1223, it would imply that the sample is underdoped. One explanation would be that samples obtained by synthesis carried out under high pressure are still underdoped, and that further oxygen doping may increase T_c. A second explanation would be that interatomic distances might play an important role. The strategy in this case would be to introduce a chemical pressure into the compound.

After completion of this work we heard that similar data had been obtained by Chu *et al.* (*10*). The two sets of data are in good agreement except that Chu *et al.* observe a saturation at 153 K ($T_{c\ \mathrm{onset}}$) around the maximum pressure attained, 15 GPa. In our case, no saturation of T_c is observed up to 23.5 GPa. Since we measure the pressure, in situ, from the lead superconducting transition, we are sure that the increase of T_c at such high temperatures is real.

REFERENCES

1. S. N. Putilin *et al.*, *Nature* **362**, 226 (1993).
2. A. Schilling *et al.*, *ibid.* **363**, 56 (1993).
3. E. V. Antipov *et al.*, *Physica C* **214** (1993).
4. N. Mori *et al.*, *ibid.* **185–189**, 40 (1991).
5. J. G. Lin *et al.*, *ibid.* **175**, 627 (1991).
6. D. D. Berkley *et al.*, *Phys. Rev. B* **47**, 5524 (1993).
7. O. Chmaissem *et al.*, in preparation.
8. M. Núñez-Regueiro, P. Monceau, A. Rassat, P. Bernier, A. Zahab, *Nature* **354**, 289 (1991).
9. L. Gao *et al.*, *Physica C* **213**, 261 (1993).
10. C. W. Chu *et al.*, *Nature*, in press.

7 September 1993; accepted 9 September 1993

Protein Enhancement of Hammerhead Ribozyme Catalysis

Zenta Tsuchihashi,* Mala Khosla, Daniel Herschlag†

When the recognition sequence of a ribozyme is extended beyond a certain length, turnover is slowed and specificity is decreased. Here, it is shown that a protein can help a ribozyme overcome these general limitations on ribozyme activity. Cleavage of an RNA oligonucleotide by a hammerhead ribozyme is enhanced 10- to 20-fold upon addition of a protein derived from the p7 nucleocapsid (NC) protein of human immunodeficiency virus–type 1. The NC protein also enhances the ability of the ribozyme to discriminate between cleavage of RNA oligonucleotides with differing sequences. These catalytic improvements can be attributed to the strand exchange activity of this RNA binding protein. It is conceivable that endogenous or added proteins may provide analogous increases in ribozyme activity and specificity in vivo.

The discovery of RNA-mediated cleavage of RNA has led to interest in the molecular and cellular function of RNA enzymes or ribozymes. The use of ribozymes to target the destruction of specific RNAs in vivo has been proposed. This approach could greatly simplify drug design because ribozymes can recognize specific RNA sequences by base pairing (*1*). However, intrinsic kinetic and thermodynamic features of ribozyme activity limit turnover and specificity. Problems arise because a recognition sequence of $\sim$15 bases is necessary to form a fully base paired duplex uniquely with a single cellular RNA (*2*). Long recognition sequences result in strong binding and slow product release for several ribozymes, thus limiting the maximal rate of turnover (*3*, *4*). Experimental work and theoretical analysis have demonstrated that strong binding also limits specificity (*5*–*7*). Binding becomes so strong that the ribozyme cleaves both a matched RNA substrate and some mismatched RNA substrates each time they bind to the ribozyme, which results in similar rates of cleavage for both matched and mismatched RNA substrates; these similar rates mean that specificity is low (*6*).

The hammerhead ribozyme HH16 (Fig. 1) provides an example of a ribozyme with slow turnover and low specificity because of strong binding (*4*, *7*). We reasoned that a protein capable of increasing the rates of helix association and dissociation could potentially enhance HH16 activity and specificity (*6*). Specifically, because binding of the RNA substrate (S) (Fig. 1) is rate-limiting for HH16 under subsaturating conditions and product dissociation is rate-limiting with saturating concentrations of S (*4*), increases in the rate of helix association and helix dissociation could increase the reaction rate under subsaturating and saturating conditions, respectively. We used the p7 nucleocapsid (NC) protein from human immunodeficiency virus (HIV) in our initial search for protein enhancement of ribozyme activity (*8*). Retroviral NC proteins are required for viral packaging and its specificity and presumably for reverse transcription, essential steps in the viral life cycle (*9*). In vitro, they can bind RNA without high specificity (*10*–*12*), mediate dimerization of the viral RNA (*13*, *14*), catalyze annealing of a transfer RNA (tRNA) primer to the viral RNA genome (*13*, *14*), and catalyze strand annealing and strand exchange with DNA oligonucleotides (*15*).

In multiple turnover reactions catalyzed by the HH16 ribozyme, there is an initial burst of product formation followed by slower product formation. The magnitude of the burst is stoichiometric with the amount of ribozyme. For example, without NC protein $\sim$10% of the 30 nM RNA substrate is rapidly converted to product by 3 nM HH16 (Fig. 2A). A detailed investigation of the rate constants of individual steps in the HH16 reaction showed that this burst corresponds to the chemical step and that the slow phase is limited by the dissociation of products, which is slower than the chemical cleavage step (*4*). However, addition of NC protein overcomes the slow phase, with the result that the entire reaction can proceed at a rate similar to that for the cleavage step (Fig. 2A) (*16*). The rate constant for the slow multiple turnover phase, k_{cat}, increases from 0.01 min^{-1} to 0.2 min^{-1} upon addition of the NC, which represents a rate enhancement of $\sim$20-fold (Fig. 2A).

Control experiments (Fig. 2B) strongly suggest that the rate enhancement arises as a result of NC protein. Only a small amount of cleavage of 5′ end-labeled substrate (S*) occurred with added ribozyme in the absence of the NC (Fig. 2B, lane 3). However, the reaction was nearly complete with added NC, and only the normal reaction product was observed (Fig. 2B, lane 4). Furthermore, incubation of S* with the NC in the absence of ribozyme gave no detectable hammerhead reaction product or degradation product (lane 2), and protease treatment abolished the enhancement of activity, as expected for a protein effector (lane 6). The enhancement was also abolished upon addition of a single-stranded DNA 28-mer (ssDNA; lanes 7 and 8); NC protein binds tightly to ssDNA (*12*, *15*). Other single-strand nucleic acid binding

---

Z. Tsuchihashi, Howard Hughes Medical Institute, Stanford University, Stanford, CA 94305.
M. Khosla and D. Herschlag, Department of Biochemistry, Stanford University, Stanford, CA 94305.

*Present address: Somatix Therapy Corporation, 850 Marina Village Parkway, Alameda, CA 94501.
†To whom correspondence should be addressed.